Measurements of Field-Aligned Currents in a Multiple Auroral Arc System

Sesiano, Jean; Cloutier, Paul A.

How to cite

SESIANO, Jean, CLOUTIER, Paul A. Measurements of Field-Aligned Currents in a Multiple Auroral Arc System. In: Journal of Geophysical Research, 1976, vol. 81, n° 1, p. 116–122. doi: 10.1029/JA081i001p00116

This publication URL: https://archive-ouverte.unige.ch/unige:154555
Publication DOI: 10.1029/JA081i001p00116

Measurements of Field-Aligned Currents in a Multiple Auroral Arc System

J. SESIANO[1] AND P. A. CLOUTIER

Department of Space Physics and Astronomy, Rice University, Houston, Texas 77001

A rocket-borne experiment to study the currents associated with a system of multiple auroral arcs was conducted at Poker Flat, Alaska, at 1122 UT on February 2, 1972. The magnetic field in the vicinity of the auroral system was measured with a cesium vector magnetometer. Possible configurations were inferred by constructing model current systems that reproduced the magnetic field variations measured along the flight path. The data are interpreted in terms of a model current system consisting of two eastward electrojets and one westward electrojet and three pairs of oppositely directed Birkeland sheet currents, all lying in a plane approximately parallel to the auroral arcs. Sheet thicknesses ranged from 20 to 60 km and current densities from 10 to 45 $\mu A/m^2$; the electrojet currents ranged from 1000 to 2000 A. A possible alternate model consisted of four pairs of sheets whose thicknesses range from 10 to 40 km with current densities from 10 to 90 $\mu A/m^2$. There was quite good agreement between the locations of the visual arcs and the upward current sheets. The overall current configuration is discussed in view of the theoretical models constructed by Atkinson and Sato and Holzer and of other observations.

INTRODUCTION

This paper reports in its central part the results of an experiment that provided information about the spatial association of a multiple auroral arc system with auroral electrojets and field-aligned currents. In the last part of the article we shall compare the observations with the theories of *Atkinson* [1970] and *Sato and Holzer* [1973]; their basic ideas are presented in the first part. We also compare this flight to the results of other Rice University auroral launches and to observations by other groups.

MODELS OF AURORAL ARC FORMATION

Before we present the results of the Nike-Tomahawk sounding rocket flight (NASA 18.111), let us review briefly two theories of multiple auroral arc formation.

Atkinson [1970] attributes the formation of multiple auroral arcs to the result of a dynamic interaction between the conductive ionosphere and the magnetosphere. Through the relative meridional motion of high-conductivity strips in the ionosphere and magnetospheric plasma sources, a modulation and a feedback oscillation are triggered. Moving flux tubes will see a time-varying magnetospheric electric field, and this will set polarization currents into motion. The magnetosphere is given a certain capacitance and the ionosphere a resistance. Field-aligned currents controlled by the ionosphere will close the circuit. Precipitating high-energy electrons will create the high-conductivity strips mentioned above, and this will close the feedback loop. Thus Atkinson considers the arcs as the standing waves in the nonlinear mode of an oscillating circuit.

Other assumptions made by Atkinson are the following: there exist north-south and east-west electric field components, though the latter one is much smaller than the former (by 1–2 orders of magnitude); the geomagnetic field lines are equipotential, which implies perfect mapping of the electric field between the magnetosphere and the ionosphere (this also leads to conjugate arcs); there is a reservoir of electrons on the inner portion of the plasma sheet, ready to be injected in the circuit; and the propagation time between the ionosphere and the magnetosphere is ignored (there is no inductance); i.e., the time for a flux tube to cross the arc (<100 s) is longer than the propagation time.

From his theory, Atkinson can estimate the following parameters for a multiple arc system: the arc width and separation, the current densities, the location of the current sheets (a broad downward current sheet, typically some tens of kilometers, beside a thin upward one, typically some kilometers, which corresponds to precipitating electrons and the visual auroral arc), and the value of the electric field components within and outside the arcs.

Single arcs can be viewed as very widely separated multiple arcs or as a case of a very heavy damping of the standing wave (the oscillation in the circuit rapidly dies out in the meridional direction).

Finally, the breakup could be explained by a northward spreading wave of proton precipitation which would enhance the electron number density inside the arc and produce the generally observed brightening from the south.

The more recent theory of *Sato and Holzer* [1973] and *Holzer and Sato* [1973] is an extension and a generalization of Atkinson's theory, but several assumptions and end results are different. Both conjugate ionospheres and the magnetosphere are involved in the circuit. Sato and Holzer assume the existence, in one ionosphere, of an electric field with a meridional component and an electron density perturbation produced, for example, by precipitation of thermal electrons from the plasma sheet; it is thin in latitude, extended in longitude, and at about 155-km altitude, where there is a low recombination rate. This dc potential in the ionospheric rest frame will be seen as an ac potential in the magnetospheric rest frame when its field lines sweep across the perturbation. Thus one ionosphere, called the 'active' one, will be the site of an ac generator. The equivalent electric circuit is more involved than Atkinson's circuit: it includes a magnetospheric inductance (i.e., there is a finite propagation time between the ionosphere and the magnetosphere) and capacitance, and a resistance in the conjugate ionosphere.

The current set into motion in the active ionosphere flows along field lines and closes in the conjugate 'passive' ionosphere. If the electron perturbation is quenched (e.g., by taking place at too low of an altitude), no auroral phenomenon will take place. If the perturbation grows, currents will circulate, and a threshold will be reached by, for example, an instability

[1] Now at Observatoire de Neuchâtel, Neuchâtel, Switzerland.

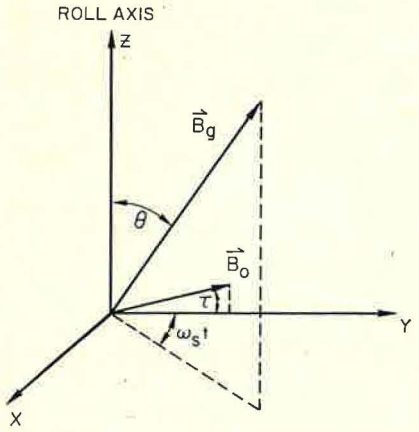

Fig. 1. Geometry for calculating the total field at the magnetometer sensor as a function of time. The z axis is parallel to the vehicle roll axis, and the coordinate system rotates with the payload at angular velocity ω_s. The bias field B_0 is fixed in the yz plane at an angle τ from the y axis, while the direction of the ambient magnetic field B_g is given by the polar angle θ and the phase angle $\omega_s t$.

of the type described by *Kindel and Kennel* [1971] and the appearance of an anomalous resistivity. The end result is a parallel electric field that will energize the electrons and give rise to a single auroral arc display at an altitude (~100–120 km) lower than where the primary perturbation took place (~155 km).

The case of two active ionospheres leads to the formation of multiple auroral arcs in the following way. In order to grow, perturbations occurring simultaneously in both ionospheres must adjust their positions so as to work coherently: the upward field-aligned current in one ionosphere will correspond to the downward current in the conjugate one. The ionosphere with the smallest recombination rate will take control of the system. The direction of appearance of successive arcs (northward or southward) will depend upon the relative magnitudes of the electric field components and the Hall and Pedersen mobilities in the E layer.

From their theory, Sato and Holzer can estimate the following quantities for a multiple arc system: the arc width and separation, the current densities, the direction of formation of each new arc (equatorward or poleward), the electrojet intensity and direction, and the location of the upward and downward current sheets (it depends upon the direction of the electric field).

The case of a single arc is inherent in the theory, since it is the basic unit that can lead by repetitive process to a multiple arc system. Conjugacy is predicted, but an arc is not necessarily associated with another one in the conjugate hemisphere.

Critical factors in their theory are the values of the Hall and Pedersen mobilities, the recombination coefficient (altitude dependent), the altitude of perturbation growth (if it is too low, it will be quenched), and the relative velocities of the electron perturbation and the magnetospheric plasma (it is linked to the induction and to the appearance of a phase lag critical to the perturbation growth).

Description of the Experiment

The magnetometer used in this experiment was an optically pumped single-cell cesium vapor scalar sensor [*Bloom*, 1962; *Ness*, 1970]. A very stable regulated current source provides a bias magnetic field with a magnitude of about 10,000 γ at an angle τ of about 10° above the rocket equatorial plane. The bias field B_0 and the ambient magnetic field B_g, making an angle θ with the rocket spin (or roll) axis, combine vectorially, and the sensor output is a signal frequency very nearly proportional to the magnitude of the total field. Spin of the vehicle (~5 Hz) produces a periodic modulation of the signal. Furthermore, the presence of a precession motion superimposes another modulation of much longer period (typically 50 s).

The geometry of our experiment is shown in Figure 1. The total field magnitude can be expressed as

$$|B(t)| = [B_g^2 + B_0^2 + 2B_gB_0(\sin\tau\cos\theta + \cos\tau\sin\theta\cos\omega_s t)^{1/2} \quad (1)$$

or

$$|B(t)| = x^{1/2}[1 - k^2\sin^2(\omega_s t/2)]^{1/2} \quad (2)$$

where

$$x = B_g^2 + B_0^2 + 2B_gB_0\sin(\theta + \tau) \quad (3)$$

$$k^2 = (4B_gB_0\sin\theta\cos\tau)/x \quad (4)$$

which in terms of frequency becomes

$$f(t) = L_{Cs}x^{1/2}[1 - k^2\sin^2(\omega_s t/2)]^{1/2} \quad (5)$$

where L_{Cs} is the first-order Larmor constant for cesium (L_{Cs} = 3.49854 Hz/γ).

Since the bias field parameters B_0 and τ can be determined accurately by calibration, the two unknowns B_g and θ can be computed by direct integration of $f(t)$ over a spin period.

The maxima of $f(t)$ occur when the bias field lies in the plane containing the ambient field and the rocket spin axis, so that variations in the azimuth ϕ of the field appear as changes in the phase of the modulated signal.

In the case of a precessing vehicle the polar angle θ and the azimuthal angle ϕ of the magnetic field exhibit a modulation at the precession period, and the expressions given above take a slightly different form. It is then more advantageous to consider a reference system fixed in the center of coning coordinate system, i.e., the direction of coning $\hat{c}$.

Thus the final measured quantities will be the ambient field magnitude B_g, its polar angle θ_c, and its azimuth ϕ_c with respect to the coning direction, i.e., a complete vector measurement.

A detailed presentation of the mathematical expressions leading to these final quantities is given by *Park and Cloutier* [1971].

The experiment package also contained an array of charged particle detectors and a lunar aspect sensor.

Launch Conditions and Geophysical Data

The payload, carried by a Nike-Tomahawk sounding rocket (NASA 18.111), was launched from Poker Flat, Alaska, at 0122 LT (1122 UT) on February 2, 1972. At the time of the launch, Kp was 2+. An average value of Kp of 3+ was measured for the three 3-hour intervals preceding the flight and for the three 3-hour intervals following the flight. The azimuth of the trajectory was within 1° of magnetic north. The rocket passed close to the zenith of Fort Yukon, 196 km north of the launch site. The apogee was 170 km at a flight time of 204 s.

Unfortunately, owing to an instrument failure, the two doors protecting the payload instrumentation were not ejected. Consequently, no data were obtained either from the particle detectors or from the lunar aspect sensor. However, a clear signal from the magnetometer was recorded from lift-off to impact. This signal indicated that vehicle stabilization (force-free precession) was achieved by about 93 s and contin-

ued until about 320 s when atmospheric drag on reentry caused perturbations. The initial coning half angle was 9.61° ± 0.01°; it increased to about 10° by 320 s. The coning period was about 53.2 s, decreasing by 0.2 s during the flight.

An attitude determination based on the magnetometer only was devised by *Sesiano* [1972]. The method is briefly as follows: from the IGRF (International Geomagnetic Reference Field) geomagnetic field expansion the angle between the field lines and the local vertical (zenith angle) is known at any point along the flight trajectory, as is the field azimuth. Taking these angles at two widely separated times during the flight and the two corresponding values of the magnetic field polar angle θ_c (defined more explicitly in the next section), it is possible to obtain the zenith angle and azimuth of the direction of coning. This method is valid if one can assume that no intense currents circulate close to the payload at the points of the trajectory chosen for this calculation.

By using the relevant quantities the total angular momentum (coning direction) elevation angle was computed to be 55.3° ± 0.1°, and its azimuth was 1° ± 2° at 95 s.

The observatory at Fort Yukon provided all-sky camera coverage, magnetic and photometric data. Only magnetic data were obtained from the observatories at Poker Flat and College because of a high cloud cover.

At the time of the launch a system of three ill-defined arcs (maximum intensity, ~20 kR) extended south of the zenith, superimposed upon a bright background (intensity, ~5 kR). Around apogee, the two southernmost arcs had merged into one broad arc of similar intensity, and the northernmost arc intensity decreased. The whole structure was spatially stable until 250 s, when the northernmost arc reintensified slightly, occupying a position about 20 km to the south of its initial one. The azimuth of the arc system was about 135°.

The magnetometer at Fort Yukon (see Figure 2) shows a 52-γ decrease in X and no deflection of the Z component at the time of the flight. This corresponds to a westward electrojet over the station. Similar behavior was exhibited by the Poker Flat and College magnetograms.

An electron number density of 5×10^9 m^{-3} was calculated for the zenith at College with data from the ionosonde located at that station; this value is slightly larger than the predicted ionospheric nighttime value [e.g., *Boström*, 1964]. This was probably due to the diffuse glow over the entire sky south of the zenith during the flight.

Experimental Results

As was previously mentioned, no data from the particle detectors were obtained, and thus only the vector magnetometer data will be presented. They are shown in Figure 3. The ΔB curve is the difference between the total ambient field (geomagnetic plus perturbation) measured at the payload and the geomagnetic field. The latter is obtained along the trajectory from the IGRF spherical harmonic expansion updated to the launch time.

The θ_c and ϕ_c curves are plots of the polar and azimuthal angles, respectively, of the total magnetic field direction in an inertial coordinate system whose polar axis is coincident with the total angular momentum (coning) direction. Once every rocket spin, these three parameters are measured. The plots in Figure 3 show an average over 10 spins, i.e., about 2 s of flight time.

Owing to the good radar acquisition of this flight we are confident that the ΔB data represent features induced by circulating currents in the vicinity of the payload. One can see that

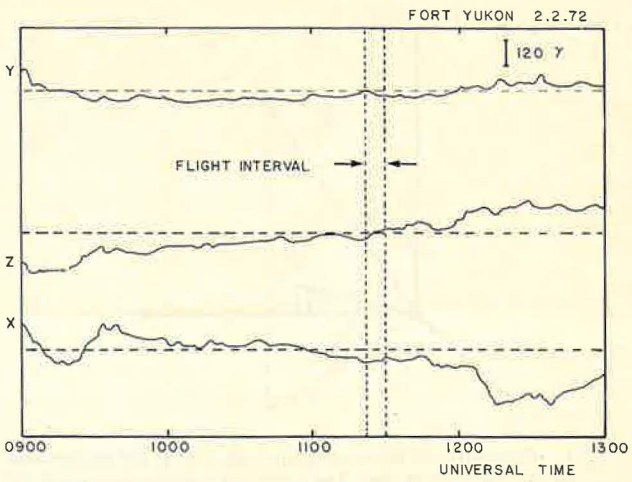

Fig. 2. The Fort Yukon magnetogram for the 4-hour interval containing the flight on February 2, 1972.

two major signals are present, well above the 2-γ noise level.

The smooth decrease of θ_c is due to the payload flying toward regions of larger dip angle. Superimposed upon it, three signals can be seen, well over the noise level of ~0.05°.

Once the linear variation due to translational motion has been removed, the azimuthal data ϕ_c show clearly three signals significant in comparison with the noise level of ~0.3°.

Interpretation of the Data

Before we present the models fitting the data, it is instructive to discuss some important points concerning the geometry of our experiments. The signals in ΔB and θ_c arise from perturbations in the meridional plane, and the signals in ϕ_c arise from perturbations in the magnetic east-west plane. Thus field-aligned currents producing a magnetic perturbation perpendicular to the geomagnetic field and in the magnetic east-west direction will affect the ϕ_c data but will alter θ_c to a lesser extent and ΔB negligibly. Conversely, the magnetic perturbation from an east-west line current lies in the meridian plane and will affect ΔB and θ_c but will leave ϕ_c unaltered. So the effect of Birkeland (field-aligned) currents is to change the direction of the geomagnetic field while it has a negligible effect on its magnitude.

The observed ΔB profile must be attributed to line currents orthogonal to the geomagnetic field. Two eastward electrojets of about 2000 A corresponding spatially to auroral arcs and a westward one of 1100 A slightly to the north of the visual auroral display (but in a region very active in the previous 30 min) could reproduce the most prominent features in ΔB (see Figure 3). These weak model line currents did not affect ϕ_c at all.

A system of field-aligned current sheets able to reproduce the ϕ_c signals was constructed. It is shown in Figure 4. It consists of three parallel pairs of current sheets having infinite extent along the east-west direction. Closing horizontal currents flow at an altitude of about 120 km. The current densities range from 10 to 45 μA/m^2 in the different sheets; these values are uncertain by about 50%. The rocket trajectory and the intensity of the 5577-Å line of O I as recorded at Fort Yukon for two different flight times are also shown. The small overlap between the second and third current sheets is probably due to a temporal variation in the intensity of the precipitating particles. There is quite a good correlation between the observed maxima of the visual display and the upward current sheets if we associate them with downward going electrons. Because of

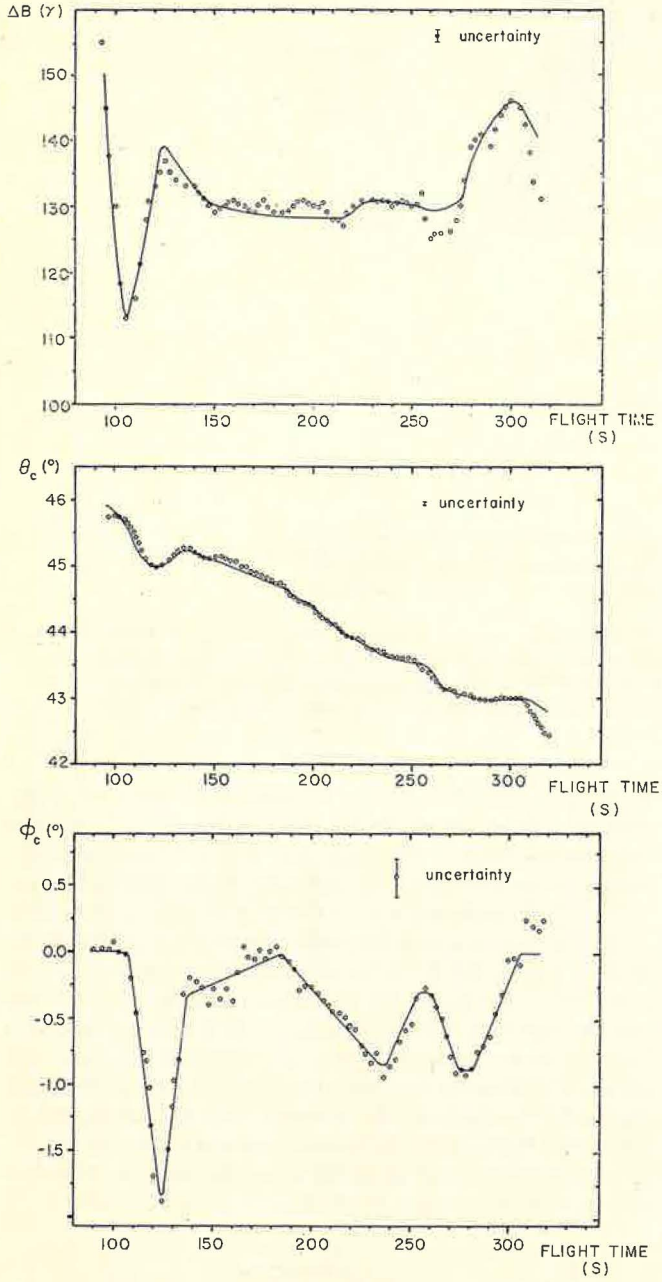

Fig. 3. Plot of the vector data obtained during the dynamically stable part of the 18.111 flight. The ΔB profile represents the magnetic field magnitude difference between the flight data and an IGRF spherical harmonic expansion. The θ_c profile represents the polar angle of the ambient magnetic field in a coordinate system centered along vehicle total angular momentum. The ϕ_c profile represents the azimuthal angle of the ambient magnetic field in a center of coning system, referred to the field position at 95 s. The error bars represent the average standard deviation, and the solid lines represent the best fit to the data when electrojets and current sheets are included.

the uncertainty in ϕ_c the current sheet boundaries can be varied by ±8 km while a reasonable fit to the data is still maintained.

As was mentioned in the previous section, the activity was widespread in the southern sky, so that the rocket penetrated part of the first auroral arc on its way up. This resulted in an uncertainty in the base line (0°) of the ϕ_c data: another base line about 0.3° lower than the one shown in Figure 3 could have been chosen. Consequently, an alternate current system capable of reproducing the ϕ_c profile was devised; it is shown in Figure 5.

It consists of four pairs of current sheets whose current densities range from 15 to 90 $\mu A/m^2$. The same uncertainties given above apply to this model.

The north azimuth of either system is 120°; it can be varied by ±10° while a relatively good fit to the data is still kept.

The two current configurations just presented reproduce well the observed data, are the simplest ones, and are the most likely on physical grounds. Because of the nonavailability of the particle data, no correlation could be made with the spatial location of the precipitating and upgoing electrons and protons.

Discussion

Two models fitting our data have been presented. We will now examine their agreement with the ground data and the predictions of the two theories discussed at the beginning of this paper.

As was mentioned above, the deflection of the Fort Yukon magnetogram can be interpreted in terms of a westward line current above that station. Furthermore, taking into account the earth currents, the magnitude of the electrojet is calculated to be about 40,000 A. This value is a little more than an order of magnitude higher than what we inferred from our magnetometer signal. The discrepancy could be explained in terms of a horizontal current sheet flowing in the highest conductivity zone of the E layer, below the altitude (~115 km, at 95 s) when data reduction started.

As has been observed by *Rostoker and Kisabeth* [1973], the eastward and westward electrojets can coexist around the midnight hours, the latter flowing north of the former. This is the geometry observed in our experiment, with an eastward circulation south of College and a westward one above and north of Fort Yukon. It has already been mentioned that there is a good spatial agreement between the upward current sheets (downgoing electrons), the eastward electrojets, and the visual auroral arcs, while the westward electrojet corresponds to a region that exhibited active auroral displays less than 30 min before the flight but was visually quiet at the time of the flight.

Let us now consider our experimental results in view of the different parameters defined by *Atkinson* [1970]. Using his constants and those of *Boström* [1964] for the conductivities and the electron number density, we obtain for a current sheet 20 km thick a current density of 5 $\mu A/m^2$, i.e., a value less than an order of magnitude smaller than the values observed during this flight. Owing to the absence of conspicuous moving features along the arc, no meridional component of the electric field could be deduced; nevertheless, a very slow southward displacement (~100 m/s) of the arc system was observed during the flight. Taking out the apparent rotation of the auroral oval over the station, a westward electric field of 5 mV/m could be inferred.

A critical parameter introduced by Atkinson in his paper is K; it depends upon the inverse of the cube of the electron number density in the arc and linearly upon the recombination rate, the arc system meridional motion, the height-integrated Pedersen conductivity, and the sheet current density I_x. For a complete description of this parameter the interested reader is referred to Appendix A. Using the constants given by Atkinson and our flight data for I_x, we compute an average value of K equal to about 2×10^8. This value, 1 order of magnitude larger than the mean value estimated by Atkinson, is still within his estimated range of variation. The other important

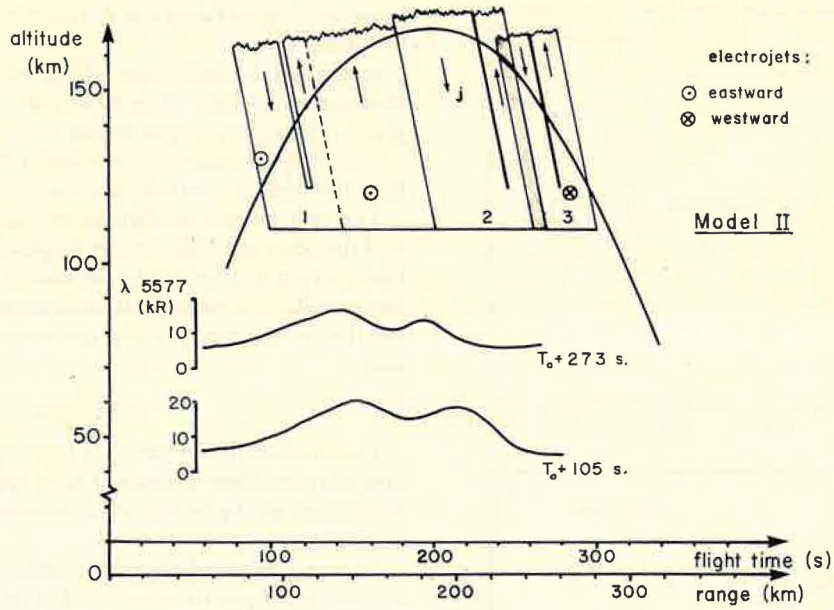

Fig. 4. A possible current system including three pairs of current sheets, two eastward electrojets, and a westward electrojet which is capable of reproducing the magnetic field changes observed during the flight. The view is in a plane perpendicular to the arc system. Arrows indicate the direction of current flow. The intensity profile of the 5577-Å line as recorded by the Fort Yukon photometer for two flight times is shown below the current system. The altitude of the horizontal closing current is assumed to be at 120 km.

parameter of Atkinson's model is f_0 (see equation (A3)), which is approximately the nondimensional meridional electric field when the east-west component is small. Its predicted range of variation goes from 3 to 100. From our observed arc parameters, f_0 ranges between 1 and 3; furthermore, using the values of K found above, we compute an arc spacing S of about 70 km versus 20–40 km for the observed values. The arc thickness σ is calculated to be 20 km versus observed values ranging from 10 to 30 km. The parameters S and σ are defined in equation (A2).

The electrojet intensity, given by (A4), is approximately 10^3 A integrated over a height of 10 km and for an electron number density of 10^{11} m^{-3}.

Finally, the electric field distribution between and inside the arcs can be estimated. We compute a meridional component that is maximum midway between the arcs (~100 mV/m); inside the arc we find a value of ~80 mV/m, which seems to be a little high in comparison with other published data. Another estimate using *Boström*'s [1964] conductivity values and our observed sheet current densities gives values around 15 mV/m, apparently closer to what has been measured [*Kelley et al.*, 1971; *Mozer and Lucht*, 1974].

In summary, we can say that Atkinson's theory is in agreement with several observed parameters. The values of the constants K and f_0 were found to be quite different from the values given in his paper but still within his predicted range of variability. On the other hand, the electric field values calculated seem too high.

Let us now look at the predictions of *Sato and Holzer*'s [1973] model. The most critical parameter in their theory is the combination $V_0 = M_P E_{0x}{}^n + M_H E_{0y}{}^n$, where M_P and M_H are the Pedersen and Hall height-averaged mobilities, respectively, and $E_{0x}{}^n$ and $E_{0y}{}^n$ are the components of the zero-order electric field in the rest frame of the neutral gas (x toward the south, y toward the east). This parameter gives the spatial distribution of the current sheets: the downward current sheet lies equatorward of the upward one if $V_0 < 0$, and vice versa if $V_0 > 0$; we note also that in their model the upward current corresponds to the visible arc. V_0 indicates also the direction of formation in a system of multiple arcs: each new arc will appear equatorward of the established ones if $V_0 < 0$ and poleward if $V_0 > 0$. Furthermore, V_0 also enters in the expression giving the current density, the electrojet intensity, the arc width, and separation. Other quantities entering in these expressions are the electron number density in the arc, the capacitance and inductance of the magnetosphere, and the resistance of the ionosphere. Let us now compare Sato and Holzer's predictions with what we observed. For the east-west electric field component the observed value of 5 mV/m will be used; with Sato and Holzer we shall assume a value of 20 mV/m for the meridional component (in the absence of such a component, their theory would lead, in our particular case, to

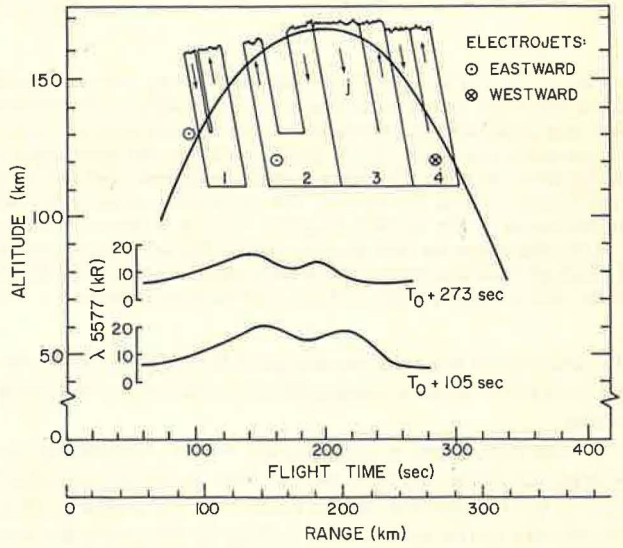

Fig. 5. Another possible current system deduced using a ϕ_c profile with the alternate base line discussed in the text.

physically unreasonable results). For the electron number density a value of 5×10^{11} m^{-3} seems reasonable in view of the brightness of the system [*Dalgarno et al.*, 1965; *Rees*, 1963]. Finally, for the mobilities we shall adopt Holzer's values (from unpublished calculations), though they seem to be too low by an order of magnitude according to the estimates of *Boström* [1964].

The wavelength λ_m (explicitly given in equations (B1) and (B2)) of the perturbation (approximately the arc spacing) is calculated to be about 3 km, and the arc width is about 1 km. Both these quantities are smaller than the observed ones by about a factor of 10. The current density (see equation (B3)) is then computed to be about 8 μA/m^2, also several times smaller than what was observed. In the calculation of the electrojet intensity an estimate of the perturbation electric field E_x^* must be made; its extreme possible values range from zero (no perturbation) to a value equal and opposite to the zero-order component E_x^0. If we adopt a value somewhere in between (i.e., $E_x^* = -(\frac{1}{2})E_x^0$ approximately), we find an electrojet intensity much too low.

Lastly, the parameter V_0 being negative, the theory forecasts a downward current sheet equatorward of the upward one; this is what was observed.

A summary of the results predicted by the two theories and of the observed values is given in Table 1.

Finally, let us present results from other rocket and satellite experiments that took place over multiple or structured arc systems; these results indeed provide further evidence for the existence of multiple field-aligned current sheets, but they also show the complexity of the problem and the possibility of different configurations at different times.

In a sounding rocket experiment at Fort Churchill, Canada, by *Choy et al.* [1971] over an active auroral display comprising bands, rays, and a bright moving fold, simultaneous measurements of the electric field and the electron fluxes were obtained; the on-board magnetometer did not have a high enough resolution to detect Birkeland currents. North of the energetic precipitated electrons responsible for the visual aurora a softer spectrum was detected (<1 keV) simultaneously with a rotation of the electric field direction from the west or southwest to the east. This configuration suggests a plasma sheet origin for the less energetic particles. Simultaneous measurements by the satellite ATS 5 at 6.6 R_E, believed to be magnetically connected to the southern edge of the auroral form, show an electron spectrum similar in shape and absolute differential intensity to that recorded by the sounding rocket. This suggests that no further acceleration mechanism is needed between the equatorial plane and the auroral ionosphere if the assumption by Choy et al. of magnetic connection is valid.

Another sounding rocket was launched at Fort Churchill by *Whalen and McDiarmid* [1972] over several east-west auroral arcs. Intense fluxes of low-energy electrons with near 0° pitch angle were detected at the northern boundary of the auroral precipitation. A current density of 200 μA/m^2 at 0.55 keV was estimated in a current sheet 10 km thick. Field alignment was observed for electrons of energy from less than a few keV to greater than 8 keV. At higher energies the electron pitch angle distribution headed toward isotropy at times of maximum fluxes, and it generally was peaked toward 90°. No significant field-aligned distributions were found south of the boundary or between the arcs. This configuration was attributed by Whalen and McDiarmid to local acceleration from a parallel electric field with a potential drop greater than 7 keV.

Very similar observations were made by *Maehlum and Moestue* [1973] with a mother-daughter sounding rocket premidnight flight over two stable auroral arcs. They were found to be imbedded in an 'ocean' of 0.5-to 3-keV field-aligned fluxes of low-energy electrons. Within the visual auroral forms the pitch angle distribution was roughly isotropic with a tendency for the 3-keV electrons to be peaked around 90°.

Additional information on the relationships of field-aligned electron fluxes, visual auroral forms, and Birkeland currents has been obtained by several other rocket flights by the Rice University group. Data were reported in the literature by *Park and Cloutier* [1971], *Vondrak et al.* [1971], and *Cloutier et al.* [1973]. They all tend to show a relationship between pitch angle and energy of the particles opposite to the one presented by Choy et al., Whalen and McDiarmid, and Maehlum and Moestue. The maximum current densities were indeed observed for the highest-energy electrons (10–20 keV), this effect being due to differences in pitch angle anisotropy. Less than 50% of the total upward current detected by the magnetometer was attributed to electrons in the energy range 0.5–20 keV. Thus it appears that both upward and downward Birkeland currents were carried by particles with energies less than 0.5 keV.

The description of these experimental data and those from our flight suggests that the high-latitude ionosphere is in nearly constant electrical contact with the magnetosphere through Birkeland currents; they are quite weak and diffuse during magnetically quiet periods but are strongly enhanced during active times.

The auroral structure observed in our experiment is of a scale much smaller than the ionospheric mapping region of the steady state quiet time Birkeland currents (several degrees in latitude). It is not yet clear if these observed auroral currents are a compression of larger auroral zone currents or if they are different entities related to a local acceleration mechanism (arising from anomalous resistivity) and superimposed on the larger auroral zone currents.

Though no particle data were obtained in the flight discussed in this paper, data from other Rice University flights tend to support the idea that the energetic electrons are not the principal current carriers, even though they are responsible for the visible emission; furthermore, they have always shown a striking spatial coincidence of the upward net Birkeland current inferred from the magnetometer with energetic electron current.

TABLE 1. Summary of Predicted and Observed Results

Parameters	Atkinson	Sato and Holzer	Observed
Arc width, km	20	1	10–30
Arc spacing, km	70	3	20–40
Meridional electric field, mV/m	80	20	15
Current density, μA/m^2	5	8	10–90
Electrojet intensity, A	1000	10	1000–2000

APPENDIX A

Taking the x axis toward the south and y toward the west, the parameter K of Atkinson's theory has the following form:

$$K = (\gamma + 1)Cv_x I_{x_0}/2\alpha e P N_1^3 \qquad \text{(A1)}$$

where γ is the electron-ion pair number created by an incoming electron (typically 100), C is the capacity of the electric circuit (typically 30 F), v_x is the velocity of flux tubes and convecting plasma as seen from our reference frame (typically

1 m/s), I_{x_0} is the x component of the ionospheric current at the origin of our reference, α is the recombination coefficient for a height-integrated electron number density N (α is typically 4×10^{-18} m^2 s^{-1}), e is the electron charge, P is a constant (typically 10^{-15} mho m^2) such that $P = \Sigma_P/N$, where Σ_P is the height-integrated Pedersen conductivity and N_1 is the perturbed height-integrated electron number density (typically 10^{15} m^{-2}).

Note also that $I_{x_0} = N_0(PE_{x_0} - H\mathcal{E}_y)$, where N_0 is the unperturbed height-integrated electron number density (typically 10^{14} m^{-2}), $H = \Sigma_H/N$ (typically 1.6×10^{-15} mho m^2), E_{x_0} is the x component of the electric field at the origin (typically 50 mV/m), and $\mathcal{E}_y = E_y - U_xB$, where E_y is the y component of the electric field in the moving frame, U_x is the velocity of the neutrals in the moving frame, and B is the geomagnetic field; $\mathcal{E}_y$ is typically 5×10^{-5} V/m.

The arc parameters are given by the following expressions:

$$\sigma = 2(K/f_0)^{1/2} \qquad S = 4(Kf_0)^{1/2} \tag{A2}$$

where the parameter f_0 is

$$f_0 = \left[\frac{(PE_{x_0} - H\mathcal{E}_y)}{(PE_{x\min} - H\mathcal{E}_y)}\right]^{1/2} \tag{A3}$$

where E_{x_0} and $E_{x\min}$ are the maximum and minimum values of E_x.

The height-integrated electrojet intensity is given by

$$I_y = N(P\mathcal{E}_y + HE_x) \tag{A4}$$

APPENDIX B

In Sato and Holzer's theory the wavelength of the perturbation is given by

$$\lambda_m = \frac{2\pi(2LC)^{1/2}v_0}{5 + 0.9(L/R^2C)} \tag{B1}$$

where L and C are the inductance and capacitance of their equivalent electric circuit (LC is typically 2.9×10^4 s^2), v_0 is the initial phase velocity of the perturbation, and R is the resistance of their circuit (L/R^2C is typically $(5 \times 10^{-21})n_0^2$, with n_0 the electron number density at the altitude of the perturbation (typically 5×10^{10} m^{-3})).

An equivalent expression for the wavelength is

$$\lambda_m = (1.6 \times 10^5)\,(E_{0x}{}^n + 0.1E_{0y}{}^n) \tag{B2}$$

where E_{0x} and E_{0y} are defined in the main body of our paper.

The maximum value of the field-aligned current density is given by

$$j_\parallel{}^m = 6.7 \times 10^{-6} \cdot \left|\frac{E_{0x}{}^n + E_{0y}{}^n(M_H/M_P)}{E_{0x}{}^n + 0.1E_{0y}{}^n}\right| \tag{B3}$$

and the maximum current flowing in the east-west (y) direction will be

$$I_y{}^m = w_x h\tilde{n}e[(\xi - 1)M_HE_{0x} + M_\xi E_{0y}] \tag{B4}$$

where w_x is the arc width given approximately by the following relation: $w_x \cong \lambda_m/\pi$; w_x is typically 4 km. Here h is the height over which we integrate (typically 30 km), $\tilde{n}$ the average electron density in the final steady state (typically 4×10^{11} m^{-3}), e the electron charge, ξ a factor between 0 and 1, and $M_\xi = (\xi M_H{}^2 + M_P{}^2)/M_P$.

Acknowledgments. We thank R. R. Vondrak and R. T. Casserly for their many contributions during the analysis and interpretation of the data. We wish to acknowledge the efforts of D. R. Oehme, A. D. White, and the other personnel of the Rice space physics facilities in the payload design, construction, launch, and data reduction. We thank the personnel of Goddard Space Flight Center and the University of Alaska who have assisted us in this project. This work was supported by contracts NAS 6-1667 and NGL-44-006-012. This paper is based on a thesis submitted by one of us (J.S.) in partial fulfillment of the requirements for the Ph.D. degree at Rice University.

The Editor thanks T. E. Holzer and T. Sato for their assistance in evaluating this paper.

REFERENCES

Atkinson, G., Auroral arcs: Result of the interaction of a dynamic magnetosphere with the ionosphere, *J. Geophys. Res., 75,* 4746, 1970.

Bloom, A. L., Principles of operation of the rubidium vapor magnetometer, *Appl. Opt., 1,* 61, 1962.

Boström, R., A model of the auroral electrojets, *J. Geophys. Res., 69,* 4983, 1964.

Choy, L. W., R. L. Arnoldy, W. Potter, P. Kintner, and L. J. Cahill, Jr., Field-aligned particle currents near an auroral arc, *J. Geophys. Res., 76,* 8279, 1971.

Cloutier, P. A., B. R. Sandel, H. R. Anderson, P. M. Pazich, and R. J. Spiger, Measurement of auroral Birkeland currents and energetic particle fluxes, *J. Geophys. Res., 78,* 640, 1973.

Dalgarno, A., I. D. Latimer, and J. W. McConkey, Corpuscular bombardment and N_2^+ radiation, *Planet. Space Sci., 13,* 1008, 1965.

Holzer, T. E., and T. Sato, Quiet auroral arcs and electrodynamic coupling between the ionosphere and the magnetosphere, 2, *J. Geophys. Res., 78,* 7330, 1973.

Kelley, M. C., F. S. Mozer, and U. V. Fahleson, Electric fields in the nighttime and daytime auroral zone, *J. Geophys. Res., 76,* 6054, 1971.

Kindel, J. M., and C. F. Kennel, Top side current instabilities, *J. Geophys. Res., 76,* 3055, 1971.

Maehlum, B. N., and H. Moestue, High temporal and spatial resolution observations of low-energy electrons by a mother-daughter rocket in the vicinity of two quiescent auroral arcs, *Planet. Space Sci., 21,* 1957, 1973.

Mozer, F. S., and P. Lucht, The average auroral zone electric field, *J. Geophys. Res., 79,* 1001, 1974.

Ness, N. F., Magnetometers for space research, *Space Sci. Rev., 11,* 459, 1970.

Park, R. J., and P. A. Cloutier, Rocket-based measurements of Birkeland currents related to an auroral arc and electrojet, *J. Geophys. Res., 76,* 7714, 1971.

Rees, M. H., Auroral ionization and excitation by incident energetic electrons, *Planet. Space Sci., 11,* 1209, 1963.

Rostoker, G., and J. L. Kisabeth, Response of the polar electrojets in the evening sector to polar magnetic substorms, *J. Geophys. Res., 78,* 5559, 1973.

Sato, T., and T. E. Holzer, Quiet auroral arcs and electrodynamic coupling between the ionosphere and the magnetosphere, 1, *J. Geophys. Res., 78,* 7314, 1973.

Sesiano, J., Rocket attitude determination using a vector magnetometer, M.S. dissertation, Rice Univ., Houston, Tex., 1972.

Vondrak, R. R., H. R. Anderson, and R. J. Spiger, Rocket-based measurement of particles, fluxes, and currents in an auroral arc, *J. Geophys. Res., 76,* 7701, 1971.

Whalen, B. A., and I. B. McDiarmid, Observations of magnetic field-aligned auroral electron precipitation, *J. Geophys. Res., 77,* 191, 1972.

(Received August 2, 1974;
accepted July 16, 1975.)